

See discussions, stats, and author profiles for this publication at: <https://www.researchgate.net/publication/260435199>

# Polyurethane Coatings Derived from 1,2,3-Triazole-Functionalized Soybean Oil-Based Polyols: Studying their Physical, Mechanical, Thermal, and Biological Properties

ARTICLE in MACROMOLECULES · OCTOBER 2013

Impact Factor: 5.8 · DOI: 10.1021/ma401554c

---

CITATIONS

10

---

READS

95

5 AUTHORS, INCLUDING:



**Shahram Mehdipour-Ataei**

Iran Polymer and Petrochemical Institute

106 PUBLICATIONS 1,214 CITATIONS

SEE PROFILE



**Atefeh Solouk**

Amirkabir University of Technology

23 PUBLICATIONS 109 CITATIONS

SEE PROFILE



**Shiva Irani**

Islamic Azad University Tehran Science and R...

28 PUBLICATIONS 174 CITATIONS

SEE PROFILE

# Polyurethane Coatings Derived from 1,2,3-Triazole-Functionalized Soybean Oil-Based Polyols: Studying their Physical, Mechanical, Thermal, and Biological Properties

Hadi Bakhshi,<sup>†</sup> Hamid Yeganeh,<sup>\*,†</sup> Shahram Mehdipour-Ataei,<sup>†</sup> Atefeh Solouk,<sup>‡</sup> and Shiva Irani<sup>§</sup>

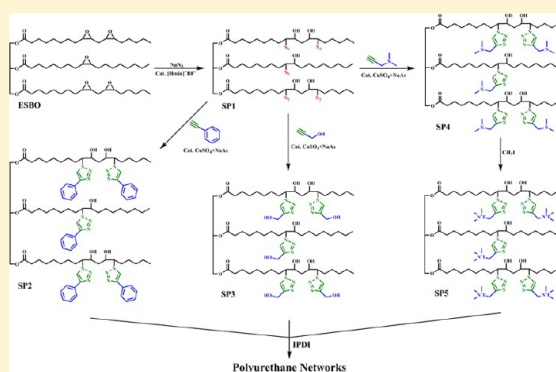
<sup>†</sup>Polyurethane Department, Iran Polymer and Petrochemical Institute, P.O. Box: 14965-115, Tehran, Iran

<sup>‡</sup>Biomedical Engineering Faculty, Amirkabir University of Technology, Tehran, Iran

<sup>§</sup>Biology Department, Science and Research Branch, Islamic Azad University, Tehran, Iran

## S Supporting Information

**ABSTRACT:** Preparation of polyurethanes derived from novel 1,2,3-triazole-functionalized soybean oil-based polyols and assessment of their possible biocidal activities were considered. Epoxidized soybean oil was reacted with sodium azide to produce an azide-containing polyol. The product was subjected to the cycloaddition reaction with various alkynes. Alkylation of *tertiary* amine-containing polyol with methyl iodide was also performed to prepare a quaternary ammonium salt (QAS)-containing polyol. The polyols and their mixtures with PEG1000 were reacted with isophorone diisocyanate to prepare polyurethane coatings. The influence of embedded functional groups on physical, mechanical, thermal and biological properties of polyurethanes was studied. Incorporation of 1,2,3-triazole groups within the polyol backbone resulted in higher storage modulus at glassy state, glass transition temperature, thermal stability and hardness of corresponding polyurethanes, while it led to lower adhesion strength and hydrophilicity. Although QAS-containing polyurethanes displayed better physical and mechanical properties, but their thermal stability were reduced. Studying the interaction of fibroblast cells with polyurethanes derived merely from oil-based polyols revealed their good cells viability (60–110%). Moderate to high biocidal activity was detected for polyols and polyurethanes containing tertiary amine and QAS groups. Improving the hydrophilicity of polyurethanes via incorporation of PEG1000 improved their biocidal activity, while it reduced their cytocompatibility.



## 1. INTRODUCTION

Because of proper physical, chemical, mechanical, and thermal performances, polyurethanes have found extensive applications as coating materials.<sup>1</sup> Generally, polyurethanes are prepared from petroleum-based raw materials; however, many scientific and industrial attempts have reported the successful replacement of these starting materials with those derived from renewable resources. The main achievement in this regard is devoted to the synthesis of polyols from vegetable oils.<sup>2,3</sup> The main driving force for this elaborate effort is mainly related to the renewability, availability, cost-effectiveness, nontoxicity and biodegradability of vegetable oil-based polyols and derived polyurethanes.<sup>4,5</sup> Regardless of castor oil with inherent hydroxyl groups, the hydroxyl functional groups should be introduced into the backbone of other vegetable oils. Many possible synthetic methods have been adapted for the incorporation of hydroxyl groups within vegetable oils structure.<sup>6–8</sup> Moreover, in some of these procedures, there is the possibility of introducing other useful functional groups into the vegetable oils backbone. For example, functional groups such as acrylate,<sup>9</sup> allyl,<sup>10</sup> azide,<sup>11–16</sup> halogens,<sup>8</sup> quaternary ammonium salts

(QASs),<sup>17,18</sup> maleate,<sup>9</sup> thiol,<sup>10</sup> and cyclic carbonate<sup>19,20</sup> have been introduced into the vegetable oils structure and utilized for further applications.

In recent years, “click” chemistry has received significant attentions. The best-known and most widely utilized reaction that fits the click chemistry concept is the copper(I)-catalyzed Huisgen [3+2] dipolar cycloaddition between azides and terminal alkynes resulting in 1,2,3-triazoles.<sup>21</sup> This reaction is high-yielding, selective, insensitive to air and moisture and can be performed both in the presence or in the absence of organic solvent.<sup>21</sup> Meanwhile, low-molecular weight 1,2,3-triazole derivatives show interesting biological properties such as antibacterial,<sup>22–25</sup> antifungal,<sup>25</sup> antiviral<sup>26</sup> antiallergic<sup>27</sup> and anticancer<sup>24</sup> activities.

Investigation of biological activities of high-molecular weight analogous of 1,2,3-triazole compounds is the main interest of the present research. Comprehensive literature survey showed

Received: July 23, 2013

Revised: September 14, 2013

Published: September 26, 2013

that although azide–alkyne cycloaddition reaction is utilized for functionalization of many materials such as dendrimers,<sup>28</sup> DNA,<sup>29</sup> microspheres,<sup>30</sup> nanoparticles<sup>31</sup> and polymers,<sup>32</sup> but possible biological activities of high-molecular weight analogous of 1,2,3-triazole-containing compounds due to the presence of 1,2,3-triazole groups have rarely been studied by scientists.<sup>33</sup> Recently, the azide–alkyne cycloaddition reaction has been used for grafting antibacterial agents such as QASs,<sup>34</sup> quaternary phosphonium salts,<sup>35</sup> peptides<sup>32</sup> and poly(2-*tert*-butylamino-ethyl methacrylate)<sup>36</sup> onto the polymeric materials. However, the observed biocidal activity of the prepared materials is related to the introduced antibacterial functions, not the 1,2,3-triazole linkers. There are other related reports regarding the application of azide–alkyne cycloaddition for the synthesis of 1,2,3-triazole-functionalized vinyl monomers<sup>37,38</sup> and preparation of linear<sup>39,40</sup> and cross-linked<sup>41,42</sup> polymers. Application of this reaction for the preparation of cross-linked polymers may suffer from the problem of catalyst entrapment within the polymer network.<sup>41,43</sup> More recently, Petrovic et al.<sup>44–46</sup> have used the values of this reaction for the preparation of cross-linked biopolymers based on azidated vegetable oils (castor, canola, corn, linseed, and soybean oils) and alkynated soybean oil under thermal conditions, without using any catalyst or solvent.

High-molecular weight compounds containing biocidal functions such as QASs, quaternary phosphonium salts and *N*-halamines have displayed more effective activity than their corresponding low-molecular weight analogous.<sup>47</sup> This phenomenon may be related to high local concentration of biocidal functions.<sup>47</sup> Therefore, it is interesting to find an insight regarding possible biocidal activity of high-molecular weight analogous of 1,2,3-triazoles. To study this subject, functionalization of soybean oil with both hydroxyl and 1,2,3-triazole groups and preparation of their corresponding polyurethane coatings were considered in this research. Soybean oil-based polyols were synthesized through azidation reaction of epoxidized soybean oil (ESBO) and subsequent reaction of this intermediate compound with different alkynes. Consequent polymerization of these functional polyols with diisocyanate monomer led to desired polyurethane coatings. The starting materials and final polymeric coatings were characterized by conventional spectroscopic methods. Physical, thermal and viscoelastic properties as well as cytocompatibility, antibacterial and antifungal properties of these newly developed materials were studied. On the basis of recorded properties, these polyurethanes can find potential applications for coating of medical devices.

## 2. EXPERIMENTAL SECTION

**2.1. Materials.** Epoxidized soybean oil (ESBO, PATSTAB 901) with a number-average molecular weight of about 1000 and epoxy content of 3.47 mmol epoxy/g was purchased from PATCHEM (Sharjah, UAE) and used as received. Sodium azide ( $\text{NaN}_3$ ), 1-methylimidazole, phenylacetylene (PhAc), propargyl alcohol (PrAl) and methyl iodide ( $\text{CH}_3\text{I}$ ) all from Merck as well as *N,N*-dimethylpropargyl amine (DMPAm) and sodium ascorbate (NaAs) from Sigma-Aldrich were used without further purification. Tetrafluoroboric acid ( $\text{HBF}_4$ , 50% w/w aqueous solution) was supplied by Acros Organics. Magnesium sulfate ( $\text{MgSO}_4$ ), sodium chloride ( $\text{NaCl}$ ), copper sulfate ( $\text{CuSO}_4$ ), ethyl acetate (EtAc) and *N,N*-dimethylformamide (DMF) all from Merck were used as received. Poly(ethylene glycol) with  $M_n = 1000$  g/mol (PEG1000), isophorone diisocyanate (IPDI) and dibutyl tin dilaurate (DBTDL) were

purchased from Merck. Tetrahydrofuran (THF) was supplied by Merck, dried over sodium wire and distilled.

Mouse L-929 fibroblast cells were supplied by CLS Cell Lines Service GmbH (Germany). *Escherichia coli* (*E. coli* PTCC 1330) as gram-negative and *Staphylococcus aureus* (*S. aureus* PTCC 1112) as gram-positive bacteria plus *Candida albicans* (*C. albicans* PTCC 5027) as fungi were received from Iranian Research Organization for Science and Technology (Iran).

**2.2. Synthesis of Ionic Liquid Catalyst.** 1-Methylimidazolium tetrafluoroborate ( $[\text{Hmim}]^+\text{BF}_4^-$ ) was prepared according to the previously reported procedure.<sup>18</sup> The details are described in the Supporting Information.

**2.3. Synthesis of Azidated Soybean Oil-Based Polyol (SP1).** Azidated soybean oil-based polyol (SP1) was synthesized via a ring-opening reaction of epoxy groups of ESBO with sodium azide using 1-methylimidazolium tetrafluoroborate as the catalyst according to the previously reported procedure<sup>13</sup> with some modifications regarding solvent type and reaction temperature. ESBO (24.0 g, 83.3 mmol epoxy),  $\text{NaN}_3$  (8.33 g, 128.2 mmol),  $[\text{Hmim}]^+\text{BF}_4^-$  (2.025 g 11.9 mmol), and DMF (20 g) were added into a 250 mL one-neck round-bottomed flask equipped with a condenser, magnetic stirrer, and oil-bath. The reaction mixture was stirred at 95 °C for 48 h. During the reaction time, samples (1 mL) were taken from the reactor at various intervals for studying the state of ring-opening reaction of epoxy groups through FTIR spectroscopy. At the end of reaction (48 h), the flask content was allowed to cool to room temperature, dissolved in ethyl acetate (100 mL), and transferred to a separatory funnel. The solution was successively washed with distilled water (100 mL) and saturated sodium chloride solution (100 mL) to remove the catalyst residue and unreacted sodium azide. The organic layer was dried over magnesium sulfate and the solvent was removed under vacuum at 40 °C. SP1 was obtained as a dark-brown and viscous liquid at 90% yield.

**2.4. Synthesis of Soybean Oil-Based Polyols Containing 1,2,3-Triazoles (SP2–SP4).** Soybean oil-based polyols containing 1,2,3-triazoles (SP2–SP4) were prepared via cycloaddition reaction of azide groups of SP1 and different alkynes using copper sulfate/sodium ascorbate as catalyst.

SP1 (10 g, 27.4 mmol azide) and PhAc (3.355 g, 32.9 mmol) or PrAl (1.844 g, 32.9 mmol) or DMPAm (2.73 g, 32.9 mmol) were dissolved in DMF/water mixture (90:10 v/v, 25 mL) in a 100 mL one-neck round-bottomed flask equipped with a magnetic stirrer. Thereafter,  $\text{CuSO}_4$  (0.437 g, 2.741 mmol) and NaAc (1.086 g, 5.482 mmol) were dissolved in DMF/water (90:10 v/v, 5 mL) and added to the flask. The reaction mixture was stirred at room temperature for 24 h. Then, the flask content was dissolved in ethyl acetate (25 mL) and transferred to a separatory funnel. The solution was successively washed with distilled water (25 mL) and saturated sodium chloride solution (25 mL) to remove the catalyst residues and unreacted alkynes. The organic layer was dried over magnesium sulfate and the solvent was removed under vacuum at 40 °C. The prepared polyols were obtained as a dark-brown and viscous liquid at 90% yield.

**2.5. Synthesis of Soybean Oil-Based Polyol Containing 1,2,3-Triazole and QAS (SP5).** Soybean oil-based polyol containing 1,2,3-triazoles and QAS (SP5) was synthesized through alkylation of SP4 with methyl iodide. For this purpose, SP4 (10 g, 23.6 mmol tertiary amine groups) and  $\text{CH}_3\text{I}$  (5.025 g, 35.4 mmol) were placed in a 100 mL round-bottomed flask equipped with condenser, magnetic stirrer and oil bath. The reaction mixture was stirred at 38 °C for 20 h. Then, the excess of methyl iodide was evaporated in a vacuum oven at 40 °C. SP5 was obtained as a dark-brown and highly viscous liquid.

**2.6. Preparation of Cross-Linked Polyurethane Coatings (XPUs).** Cross-linked polyurethane coatings (XPUs) were prepared via one-shot reaction of polyols with IPDI monomer. The quantities of ingredients for each formulation are given in Table 1. As a general procedure, the desired amounts of polyols and catalyst (DBTDL) were dissolved in moisture-free THF solvent. Then IPDI monomer was added and solid content was fixed to 35 wt %. The solution was stirred vigorously at room temperature and degassed via application of mild vacuum. Free standing films of polyurethanes with final thickness of about 0.5 mm were prepared by casting the monomers solution in a

Table 1. Different Formulations of Polyurethanes.<sup>a</sup>

sample code	polyols type	polyols weight (g)	IPDI weight <sup>b</sup> (g)	DBTDL (g)	gel content (%)
XPU-A1	SP1	4.0	1.284	$1.2 \times 10^{-2}$	$98.3 \pm 1.5$
XPU-A2	SP2	4.0	0.991	$1.2 \times 10^{-2}$	$99.4 \pm 0.5$
XPU-A3	SP3	4.0	2.089	$1.2 \times 10^{-2}$	$99.3 \pm 0.6$
XPU-A4	SP4	4.0	1.035	$1.2 \times 10^{-2}$	$95.2 \pm 1.8$
XPU-A5	SP5	4.0	0.776	$1.2 \times 10^{-2}$	$92.3 \pm 2.1$
XPU-B2	SP2/ PEG1000	2.8/1.2	0.960	$1.2 \times 10^{-2}$	$97.4 \pm 1.2$
XPU-B3	SP3/ PEG1000	2.8/1.2	1.729	$1.2 \times 10^{-2}$	$99.5 \pm 0.5$
XPU-B4	SP4/ PEG1000	2.8/1.2	0.991	$1.2 \times 10^{-2}$	$99.5 \pm 0.5$
XPU-B5	SP5/ PEG1000	2.8/1.2	0.810	$1.2 \times 10^{-2}$	$93.5 \pm 2.5$

<sup>a</sup>XPU: cross-linked polyurethane. SP: soybean oil-based polyol. PEG1000: poly(ethylene glycol) 1000. IPDI: isophorone diisocyanate. DBTDL: dibutyl tin dilaurate. <sup>b</sup>[NCO]/[OH] = 1/1.

Teflon mold ( $10 \times 10 \times 0.2 \text{ cm}^3$ ). For evaluating the adhesion strength of polyurethanes, the monomers solution was also poured on a surface-treated aluminum plate (aluminum alloy 1050,  $10 \times 5 \text{ cm}^2$ ) and spread them with a doctor blade ( $200 \mu\text{m}$ ). The surface treatment procedure included washing of the plates with acetone, sinking them in NaOH solution (0.1 M) for 2 h and neutralizing them with HCl solution (0.01 M). The curing reaction was continued at  $70^\circ\text{C}$  for 8 h. All samples were kept at  $90^\circ\text{C}$  for 1 h for postcuring stage.

**2.7. Instruments.** <sup>1</sup>H NMR spectra were recorded on a 400 MHz Bruker instrument (model Avance 400, Germany) at room temperature using  $\text{CDCl}_3$  as a solvent. FTIR spectra were recorded on a Bruker instrument (model Aquinox 55, Germany) in the range of  $4000\text{--}400 \text{ cm}^{-1}$  at a resolution of  $0.5 \text{ cm}^{-1}$  and signal averaged over 8 scans.

Dynamic mechanical analysis (DMA) was carried out on a Triton instrument (model Tritec 2000, England) in torsion mode, temperature range of  $-50$  to  $300^\circ\text{C}$ , heating rate of  $5^\circ\text{C}/\text{min}$  and frequency of 0.1, 1, and 10 Hz. The values of storage modulus ( $G'$ ), loss modulus ( $G''$ ) and loss tangent ( $\tan \delta$ ) versus temperature were recorded for each sample. The maximum temperature of  $\tan \delta$  curves was considered as glass transition temperature ( $T_g$ ) of samples. Differential scanning calorimetry (DSC) was carried out on a Netzsch instrument (Model 200F-3 Maia, Germany). Small piece of each sample ( $\sim 20 \text{ mg}$ ) was put into aluminum vessels and heated from  $-50$  to  $+200^\circ\text{C}$  at a heat rate of  $10^\circ\text{C}/\text{min}$  under nitrogen atmosphere. The  $T_g$  values were estimated as the temperatures at the inflection-point of the change in the baseline.

Thermogravimetric analysis (TGA) was carried out on a Mettler-Toledo instrument (model TGA/DSC 1, Switzerland) from 25 to  $600^\circ\text{C}$  at a heat rate of  $10^\circ\text{C}/\text{min}$  under nitrogen atmosphere. Scanning electron microscopy (SEM) was carried out on a Tescan instrument (model Vega II, Czech) to study the morphological properties of fibroblast cells attached to the polyurethanes. The samples were placed on specimen holders using double-sided tape and coated with gold prior to use.

Hardness of prepared samples was determined by a pendulum hardness tester (Elcometer, model 3034, England) on persoz mode according to ASTM D4366 test method. Adhesion strength of polyurethanes on a surface-treated aluminum substrate (aluminum alloy 1050) was also studied by a pull-off adhesion tester (Erichsen Testing Equipments, model 525, USA) according to ASTM D4541 test method.

**2.8. Measurements.** The hydroxyl number ( $\text{OH}^\#$ ) and acid number ( $\text{AC}^\#$ ) of the prepared polyols were determined according to ASTM D4274 and ASTM D4662 test methods, respectively. For determining the gel content of polyurethane networks, samples were weighed accurately and extracted by THF in a Soxhlet extractor for 24 h. The insoluble part was dried at  $70^\circ\text{C}$  and weighed. The gel content was defined as follows:

$$\text{gel content \%} = (W_d/W_i) \times 100 \quad (1)$$

where  $W_d$  was the weight of dried sample after extraction and  $W_i$  was the initial weight of the sample. The values reported were an average of three measurements.

Cross-link density ( $\nu_c$ ) of the polyurethanes was estimated from their storage modulus in the rubbery region by applying an equation from the statistical theory of rubber elasticity.<sup>48</sup>

$$G' = \Phi \nu_c RT \quad (2)$$

where  $G'$  was the storage shear modulus at the onset of the rubbery plateau region obtained from DMA curves,  $\Phi$  as the front factor that was taken as 1 for ideal rubber,  $\nu_c$  as the cross-link density, defined as the mole number of network chains per unit volume of the polymer,  $R$  as the gas constant, and  $T$ , the absolute temperature at the beginning of the rubbery plateau region.

Surface hydrophilicity of polyurethanes was determined by measurement of water droplet contact angle. Six water droplets were placed at different positions of the surface of samples. The contact angle was determined via running ImageJ 1.44p software on the digital pictures taken from interfaces of films and droplets. The values reported were an average of six measurements.

The bulk hydrophilicity of samples was evaluated based on equilibrium water absorption (EWA) of samples in distilled water and PBS. The completely dried and accurately weighed samples were soaked in distilled water or PBS at room temperature until the equilibrium was attained (about 96 h). The weights of swollen samples were determined after blotted with filter paper to remove the surface liquid. EWA was calculated using the following equation:

$$\text{EWA (\%)} = [(W_s - W_d)/W_d] \times 100 \quad (3)$$

Here  $W_d$  and  $W_s$  are the weights of dry and swollen samples, respectively. The values reported were an average of three measurements.

**2.9. Cytocompatibility Assays.** Cytocompatibility of the prepared polyurethanes was studied by either microscopic investigation of L929 mouse fibroblast cells morphology after direct contact with samples or tetrazolium dye-based colorimetric assay (MTT assay) according to our previously reported procedures.<sup>17,18,49,50</sup> Samples were initially washed and extracted with ethanol/water mixture (70:30 v/v) for 1 week to remove all nonbonded compounds. The percentage of relative cell viability was calculated according to following equation:

$$\text{cell viability \%} = \frac{\text{OD}_{\text{sample}} - \text{OD}_{\text{negative control}}}{\text{OD}_{\text{positive control}} - \text{OD}_{\text{negative control}}} \times 100 \quad (4)$$

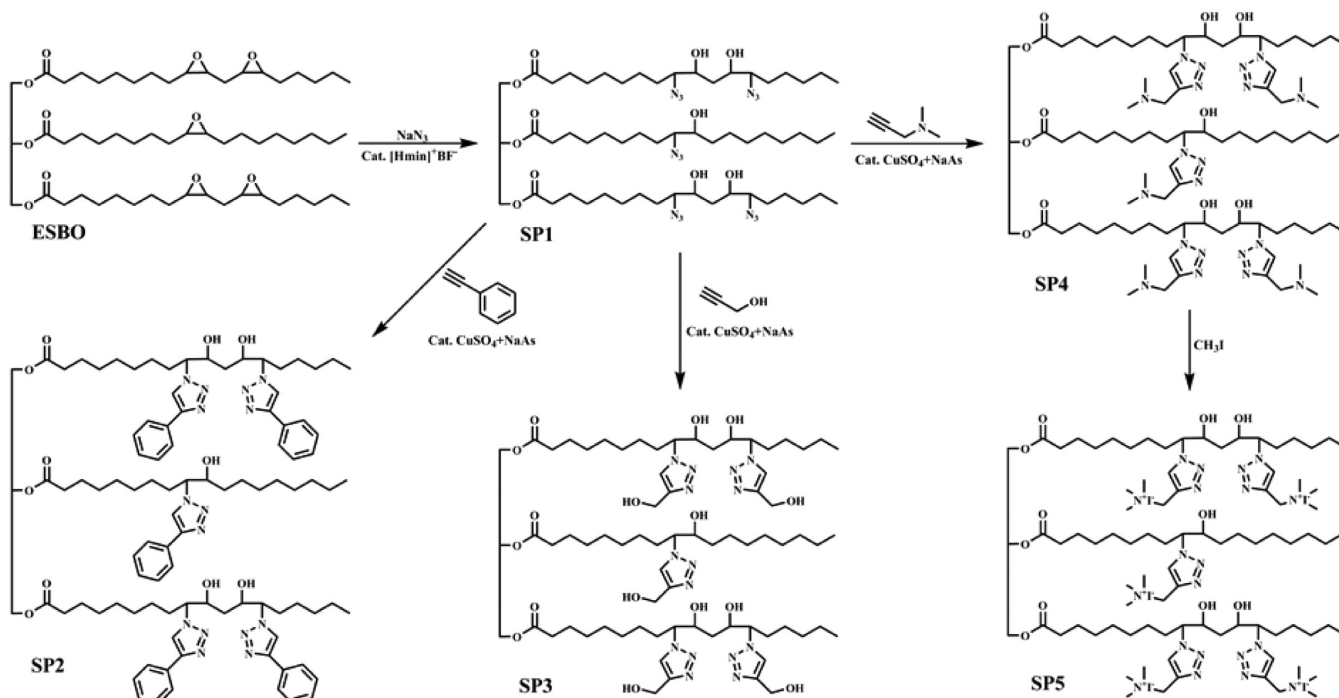
, where OD was the optical density.

To prepare samples for SEM observation, at the end of incubation (24 h), samples were washed with PBS to remove unattached cells. The adhered cells were then fixed by glutaraldehyde solution (2.5%) for 10 min and dehydrated through a series of ethanol/water mixtures (10, 30, 50, 70, 80, 90, and 100%) each for 10 min. Dehydration was followed by air drying overnight.

**2.10. Antibacterial and Antifungal Assays.** Antibacterial and antifungal activities of polyols and polyurethanes were studied against *E. coli* PTCC 1330, *S. aureus* PTCC 1112, and *C. albicans* PTCC 5027 through agar diffusion and shaking flask methods according to our previously reported procedures.<sup>17,18,49,50</sup> The samples were first washed and extracted with ethanol/water mixture (70:30 v/v) for 1 week. The percentage of microorganism reduction was calculated according to the following equation:



Scheme 1. Synthetic Route for the Preparation of Functional Polyols from ESBO



microorganism reduction %

$$= \left( 1 - \frac{\text{OD}_{\text{sample}} - \text{OD}_{\text{positive control}}}{\text{OD}_{\text{negative control}} - \text{OD}_{\text{positive control}}} \right) \times 100 \quad (5)$$

, where OD was the optical density.

**2.11. Statistical Analyses.** Statistical analyses were performed via PASW Statistics program package, version 18 (SPSS Inc., Chicago, IL). Comparison of the obtained data for different samples was performed with One-Way ANOVA with Tukey or Bonferroni posthoc tests. The significance level was set at  $p \leq 0.05$ .

### 3. RESULTS AND DISCUSSIONS

The general objective of this research was the functionalization of soybean oil with hydroxyl and 1,2,3-triazole groups and utilization of these materials as functional polyols for the preparation of polyurethane coatings. For this propose, an azidated soybean oil was prepared from the reaction of sodium azide with ESBO using 1-methylimidazolium tetrafluoroborate as catalyst. This material (SP1) was subjected to the cycloaddition reaction with various alkynes to produce 1,2,3-triazole-functionalized polyols (SP2–SP4). Copper sulfate and sodium ascorbate were used as catalyst couple. After completion of reaction the prepared materials were washed with water and saturated sodium chloride solution to remove the catalyst residue. Therefore, the final coating materials were free from colored toxic copper salt. In order to study the possible antibacterial property of QAS-containing coatings, the alkylation of *tertiary* amine-containing polyol (SP4) with methyl iodide was considered to the preparation of SP5. The outline of reactions leading to functional polyols is presented in Scheme 1.

**3.1. Synthesis and Characterization of Functional Polyols.** Different strategies were followed for the introduction of azide functionality into the fatty acid chains of vegetable oils. Metzger et al.<sup>14,15</sup> have performed the azidation reaction of methyl esters of epoxidized castor, epoxidized linseed,

epoxidized sun flower and vernolic oils using ammonium chloride ( $\text{NH}_4^+\text{Cl}^-$ ) as catalyst and ethanol/water mixture as reaction medium at reflux condition. Adewuyi et al.<sup>12</sup> have also used ammonium chloride as catalyst for azidation of methyl ester of epoxidized *Hura crepitans* seed oil in DMF at 60 °C. Manganese(III) acetate induced radical addition of azide to internal  $\text{C}=\text{C}$  bonds of sun flower oil has also been reported by Metzger et al.<sup>11,16</sup> Biswas et al.<sup>13</sup> used 1-methylimidazolium tetrafluoroborate as environmentally friendly catalyst for azidation of epoxidized methyl oleate, epoxidized methyl linoleate and ESBO in water media at 65 °C. This catalyst and the same reaction condition were repeated by us for azidation of ESBO. FTIR spectrum of the product showed low conversion of epoxy groups even after 72 h of reaction duration or increasing the concentrations of either sodium azide or catalyst (data is not shown). Although increasing the reaction temperature up to 95 °C improved the conversion of epoxy rings, but the FTIR spectrum of this product showed considerable reduction of ester carbonyl peak at  $1743\text{ cm}^{-1}$  and appearance of a new peak at about  $1670\text{ cm}^{-1}$ . This new peak could be attributed to hydrolysis reaction of ester groups and production of acylazide groups. Therefore, we modified this procedure and performed the reaction in DMF instead of water at 95 °C. Monitoring the FTIR spectra of samples collected from reaction mixture confirmed the complete consumption of epoxy rings at about 48 h, while the ester linkages were remained intact. More details regarding follow up of this reaction are given in Supporting Information (Figure S1). The structure of SP1 was also studied by  $^1\text{H}$  NMR and FTIR spectroscopy (Supporting Information, Figure S2). The amount of unreacted epoxy groups of ESBO was determined via comparing the integration value of peaks related to the protons of epoxy groups (2.7–3.1 ppm) and methane proton (5.1 ppm) of the glycerol moiety of ESBO. On the basis of  $^1\text{H}$  NMR data 93.3% conversion of epoxy groups was achieved under the applied condition of ring-opening reaction of epoxy

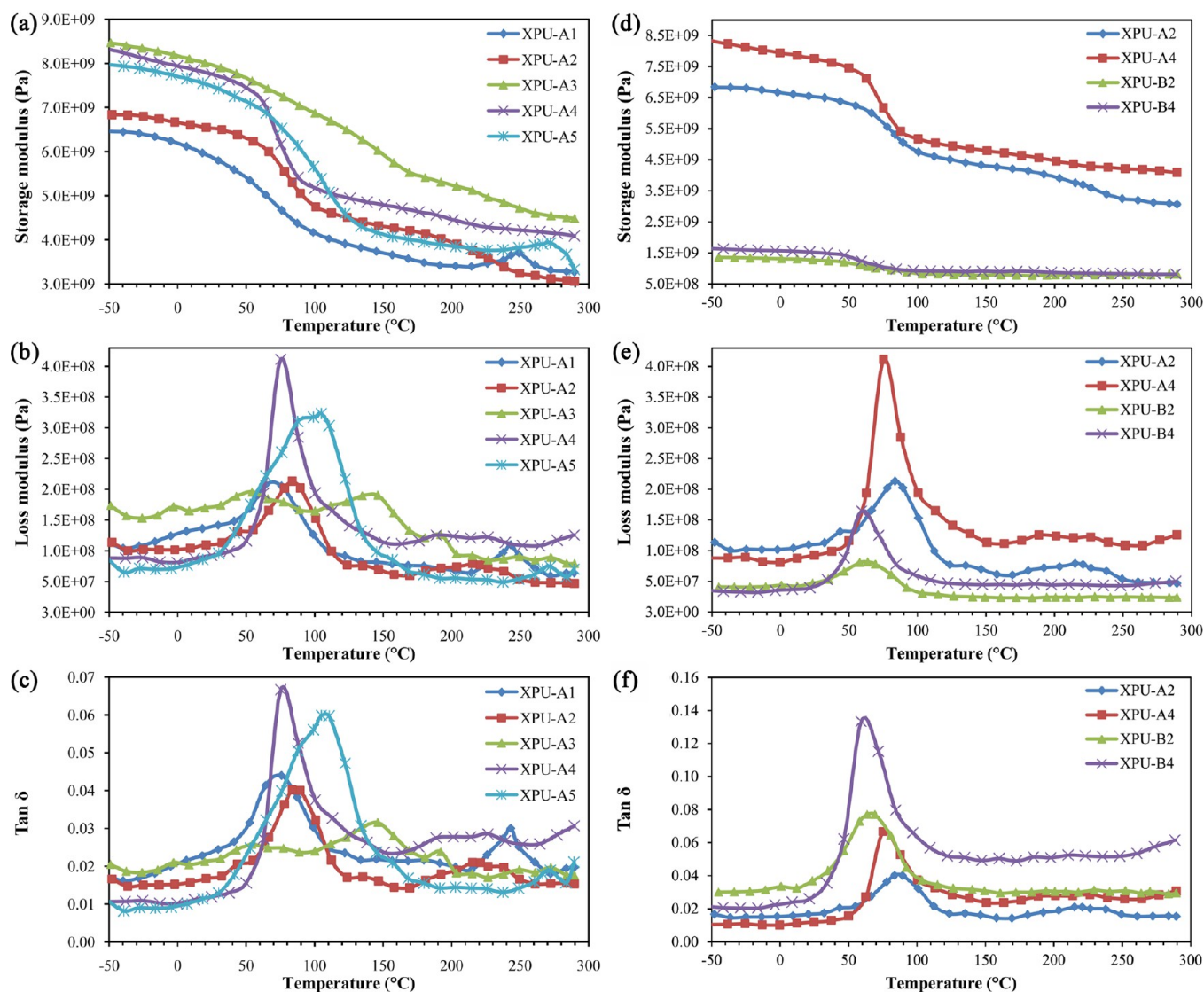


Figure 1. Storage modulus (a, d), loss modulus (b, e), and  $\tan \delta$  (c, f) vs temperature curves for polyurethanes.

Table 2. DSC and DMA Data of Polyurethanes

sample code	$E'$ at glassy state (MPa) $\times 10^{-3}$	$T_g$ (°C)		$T_{gh}$ (°C) DMA	$\tan \delta$ at $T_g$	$E'$ at the onset of rubbery region (MPa) $\times 10^{-3}$	temperate at the onset of rubbery region (K)	$\nu_c$ (mol/m <sup>3</sup> ) $\times 10^{-5}$
		DMA	DSC					
XPU-A1	6.47	73	55	—	0.044	3.83	406	11.34
XPU-A2	6.84	85	70	220	0.040	4.59	395	13.98
XPU-A3	8.47	146	113	249	0.032	5.4	453	14.37
XPU-A4	8.33	79	68	226	0.067	4.79	424	13.59
XPU-A5	7.97	106	89	—	0.060	4.17	418	11.99
XPU-B2	1.36	64	44	—	0.077	0.83	376	2.65
XPU-B3	ND <sup>a</sup>	ND	59	ND	ND	ND	ND	ND
XPU-B4	1.65	59	47	—	0.133	0.93	370	3.03
XPU-B5	ND	ND	60	ND	ND	ND	ND	ND

<sup>a</sup>Data is not available.

groups of ESBO with sodium azide, which is comparable with Biswas et al.<sup>13</sup> results.

The chemical identity of polyols (SP2–SP4) obtained from cycloaddition reaction of SP1 with various alkynes was also evaluated by <sup>1</sup>H NMR and FTIR spectroscopy. These data confirmed complete conversion (95–98%) of azide groups of

SP1 during cycloaddition reaction. Moreover, based on spectroscopic findings no side products were detected in the final polyols. For SP5, the yield of alkylation reaction was calculated as 80% by <sup>1</sup>H NMR data. Since an excess of methyl iodide was used in the course of alkylation reaction of tertiary amine groups of SP4, some of 1,2,3-triazole groups were

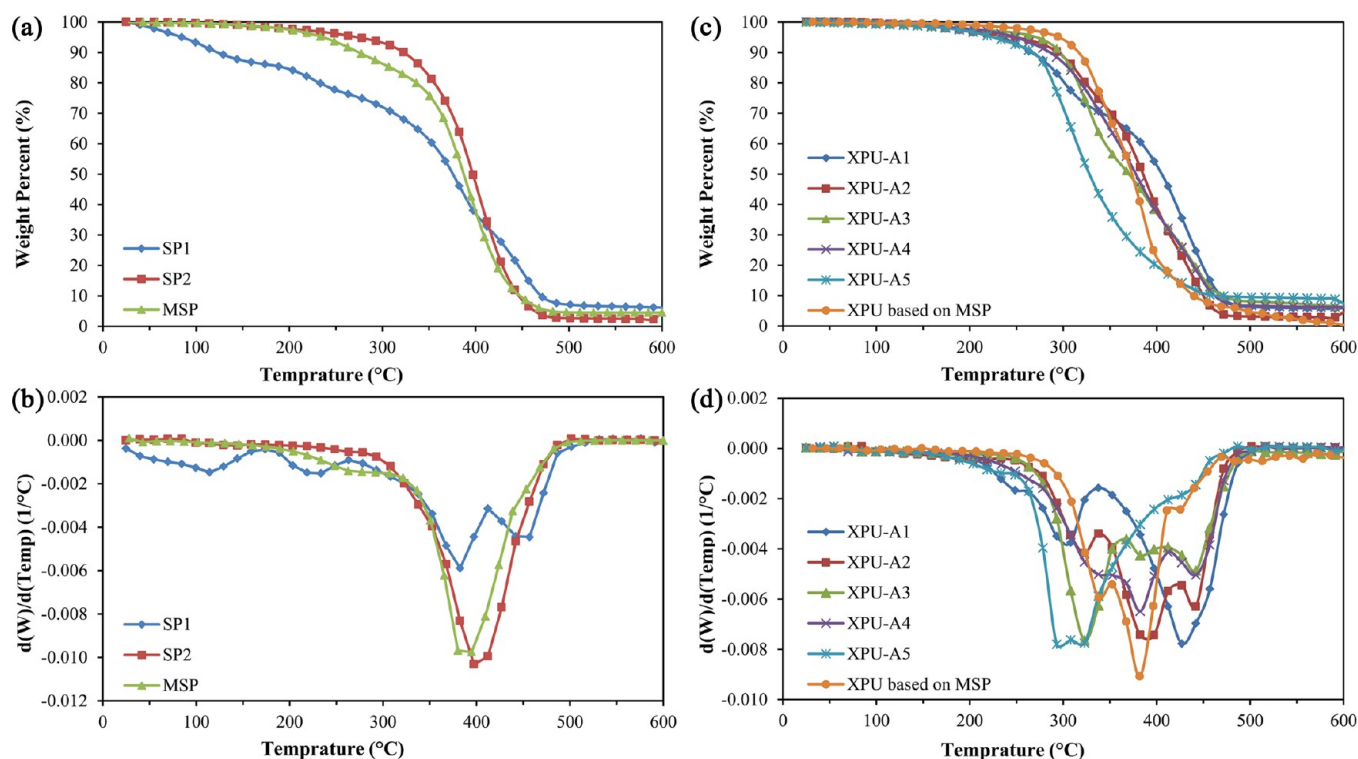


**Figure 2.** TGA (a, c) and DTGA (b, d) curves for polyols and polyurethanes. MSP was synthesized from the reaction of ESBO and methanol.<sup>18</sup> XPU based on MPS was prepared from the reaction of MSP and IPDI.<sup>18</sup>

**Table 3.** Hydrophilicity, Hardness, and Adhesion Strength of Polyurethanes<sup>a</sup>

sample code	contact angle ( $\theta$ , deg)	EWA (%)		pendulum hardness ( $s^{-1}$ )	adhesion strength (MPa)
		in distilled water	in PBS		
XPU-A1	$43 \pm 1^a$	$24.9 \pm 1.1^a$	$25.4 \pm 1.2^a$	$219 \pm 4^a$	$0.27 \pm 0.03^a$
XPU-A2	$83 \pm 2^b$	$2.5 \pm 0.5^b$	$1.4 \pm 0.1^b$	$234 \pm 7^{b,c}$	$0.21 \pm 0.01^b$
XPU-A3	$82 \pm 2^b$	$1.5 \pm 0.2^b$	$1.2 \pm 0.5^b$	$355 \pm 2^d$	$0.14 \pm 0.02^c$
XPU-A4	$75 \pm 1^c$	$9.1 \pm 1.0^{b,c}$	$8.4 \pm 0.1^b$	$226 \pm 4^b$	$0.22 \pm 0.01^{a,b}$
XPU-A5	$64 \pm 1^{d,e}$	$64.4 \pm 5.0^d$	$58.4 \pm 5.1^c$	$288 \pm 8^c$	$0.43 \pm 0.03^d$
XPU-B2	$73 \pm 2^{c,f}$	$22.4 \pm 3.2^a$	$18.7 \pm 3.8^a$	$156 \pm 6^f$	—
XPU-B3	$72 \pm 1^f$	$15.0 \pm 0.7^{a,c}$	$8.2 \pm 2.1^b$	$248 \pm 5^g$	—
XPU-B4	$67 \pm 2^c$	$18.8 \pm 2.2^{a,c}$	$17.7 \pm 2.0^a$	$139 \pm 8^h$	—
XPU-B5	$61 \pm 1^d$	$104.6 \pm 8.8^e$	$82.3 \pm 4.2^d$	$196 \pm 5^c$	—

<sup>a</sup>According to analysis of variances the difference between quantities with similar superscripts (*a, b, c, d, e, f, g* and *h*) is not significant ( $p > 0.05$ ) for data of each column.

converted into the 3-methyl-1,2,3-triazolium iodide.<sup>51</sup> The spectra and related details of synthesized 1,2,3-triazole-functionalized polyols are given in Supporting Information (Figure S3–S6).

To use the prepared polyols for the preparation of polyurethanes, it was necessary to determine the equivalent weight (EW) of polyols. The measured OH numbers were 162, 125, 279, 131, and 98 mg KOH/g for SP1, SP2, SP3, SP4, and SP5, respectively. These values corresponded to equivalent weights of 346, 448, 201, 429, and 571 g/mol, respectively.

**3.2. Synthesis and Characterization of XPUs.** Polyurethane coatings were prepared via reaction of synthesized functional polyols with IPDI monomer at [NCO]/[OH] molar ratio of 1/1 under optimum condition (Table 1). Polyurethanes derived from aliphatic diisocyanates have several benefits such as high durability and no carcinogenic degradation production in comparison to those obtained from aromatic diisocyanates.<sup>1</sup> Therefore, IPDI has been chosen for the preparation of

polyurethanes. To control the hydrophilicity of the final polyurethanes, in some of formulations, 30 wt % of soybean oil-based functional polyols was replaced by PEG1000. All of the prepared polyurethanes showed complete curing with gel content of above 92%. Considering the structure of soybean oil-based polyols with secondary hydroxyl groups and bulky dangling chains, which can restrict the formation of urethane bonds, the recorded gel content for polyurethane networks was reasonable. It confirmed that the thermal curing procedure was adequate for successful cross-linking reaction of hydroxyl and isocyanate groups. The low amount of sol fraction may be related to unreacted or partially reacted polyol residues.

The structure of the polyurethanes was confirmed by FTIR spectroscopy (Supporting Information, Figure S7). The absence of peaks related to isocyanate and hydroxyl groups at 2270 and  $\sim 3450\text{ cm}^{-1}$  and high gel content of cured samples (Table 1) confirmed almost complete reaction of these reactive groups. Furthermore, the main peaks related to oil backbone



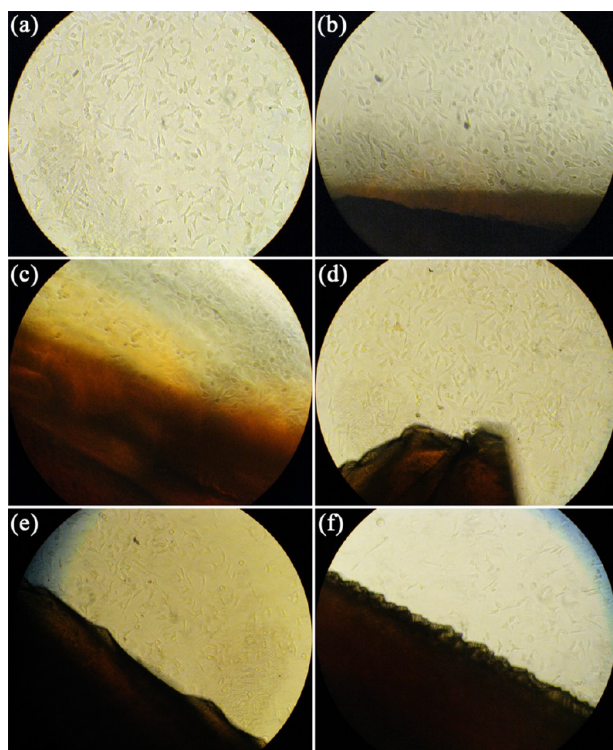


**Figure 3.** Optical microscopy images of L929 mouse fibroblast cells in direct contact with washed polyurethanes after 24 h incubation: XPU-A1 (a), XPU-A2 (b), XPU-A3 (c), XPU-A4 (d), XPU-A5 (e), XPU-A6 (f), and cells without sample (g).

and 1,2,3-triazole groups remained intact in the final polyurethanes.

### 3.3. Viscoelastic and Thermal Properties of XPUs.

Thermal transitions and relaxations related to the structure and morphology of prepared polyurethanes were analyzed using DMA and DSC techniques. The variation in storage modulus ( $G'$ ), loss modulus ( $G''$ ) and loss tangent ( $\tan \delta$ ) as a function of temperature was monitored and the results are shown in Figure 1. The thermal transition temperatures and calculated cross-link density of polyurethane networks are also collected in Table 2.

According to Figure 1, samples made solely from functional polyols (polyurethanes series A, XPU-As) showed different thermo-mechanical behaviors. XPU-A1 showed an one-phase structure, since just one peak was observed at 73 °C in  $\tan \delta$  and loss modulus curves, meanwhile a decrease in storage modulus was detected. Since this transition shifted to higher temperature upon increasing the frequency from 0.1 to 10 Hz, it was considered as glass transition phenomenon ( $T_g$ ). The data of a polyurethane derived from a methoxy functional soybean oil-based polyol (MSP) and IPDI<sup>18</sup> was considered and a one-phase structure ( $T_g = 50$  °C) was detected. Therefore, the peak observed at about 240 °C in  $\tan \delta$  and loss modulus curves of XPU-A1 and corresponding increase of storage modulus could be related to the extra cross-linking of network originated from azide groups. Thermal degradation of azide groups, production of highly reactive nitrene ( $-N:$ ) species, abstracting hydrogen atoms from aliphatic backbone of soybean oil, subsequent generation of carbon centered radical, and finally coupling of these radicals were considered as the main synthetic events occurring during extra cross-linking reactions.<sup>52–54</sup>

Samples XPU-A2–4 displayed a two-phase structure as two peaks were observed in their  $\tan \delta$  and loss modulus curves. The first transition in the range of 79–146 °C was related to the glass transition phenomenon of soft segments ( $T_{gs}$ ) originated from fatty ester structure of soybean oil. The second transition was associated with the hard segments consisting of urethane and 1,2,3-triazole groups with glass transition ( $T_{gh}$ ) in the range of 220–249 °C. Comparing the DMA data of these samples with those recorded for a polyurethane based on MSP and IPDI,<sup>18</sup> indicated that the 1,2,3-triazole groups are responsible for the formation of the two-phase structure and corresponding hard segment glass transition phenomenon. Although, the overall content of hard segments was not too high, but it was likely that the dipole–dipole interactions of aromatic 1,2,3-triazole groups were strong enough to form a second phase.

XPU-A5 showed an one-phase structure, since one peak was observed at 106 °C in  $\tan \delta$  and loss modulus curves. The sharp decrease of storage modulus and partial increase of  $\tan \delta$  at about 270 °C was related to the thermal decomposition of incorporated QAS (alkyltrimethylammonium iodide and 3-methyl-1,2,3-triazolium iodide) moieties.<sup>55–60</sup> QAS groups are known to decompose through a combination of dealkylation and Hoffman elimination mechanisms.<sup>54,55,57</sup>

For polyurethanes made from mixture of soybean oil-based functional polyols and PEG1000 (polyurethanes series B, XPU-Bs), a single phase structure with a glass transition temperature in the range of 59–64 °C was detected. It seems the presence of PEG1000 with higher polarity was responsible for phase mixing and increased domains cohesion in final polyurethanes.

For XPU-As, the highest storage modulus at glassy state was detected for XPU-A3 (Figure 1a), which was made from SP3. This was attributed to higher cross-link density ( $\nu_c = 1.437 \times 10^6$  mol/m<sup>3</sup>) of this sample arising from higher hydroxyl number ( $OH^{\#} = 279$  mg KOH/g) of SP3. Furthermore, the higher storage modulus at glassy state of XPU-A4 in comparison to XPU-A2 and XPU-A5 may be attributed to the higher cross-link density ( $\nu_c = 1.359 \times 10^6$  mol/m<sup>3</sup>) of this sample as well as the presence of polar tertiary amine groups with possible intermolecular dipole–dipole interactions. The bulky and secondary nature of hydroxyl groups of polyols can restrict the formation of urethane bonds. Embedded tertiary amine groups in SP4 can facilitate the reaction of hydroxyl and isocyanate groups. Therefore, the cross-link density of XPU-A4 is higher in comparison to XPU-A2 and XPU-A4. Detecting lower cross-link density ( $\nu_c = 1.199 \times 10^6$  mol/m<sup>3</sup>) for XPU-A5 prepared from SP5 strengthened the above given hypothesis, since after alkylation reaction of tertiary amines, no extra catalytic effect could be preserved on the reaction of hydroxyl and isocyanate groups. All of polyurethanes consisting of PEG1000 (XPU-Bs) showed lower cross-link density in comparison to corresponding formulations made merely from soybean oil-based functional polyol (XPU-As). This phenomenon was related to the lower hydroxyl number of PEG1000 ( $OH^{\#} = 112$  mg KOH/g) in comparison to soybean oil-based functional polyols.

Investigation of DMA results also showed highest  $T_{gs}$  value (249 °C) for a sample made from SP3 (XPU-A3), which was again related to lower degree of freedom of chain segments as a result of its higher cross-link density. XPU-A5 also showed high  $T_{gs}$  value due to higher ionic interactions and therefore stronger physical cross-linking originated from its QAS (alkyltrimethylammonium iodide and 3-methyl-1,2,3-triazolium iodide)



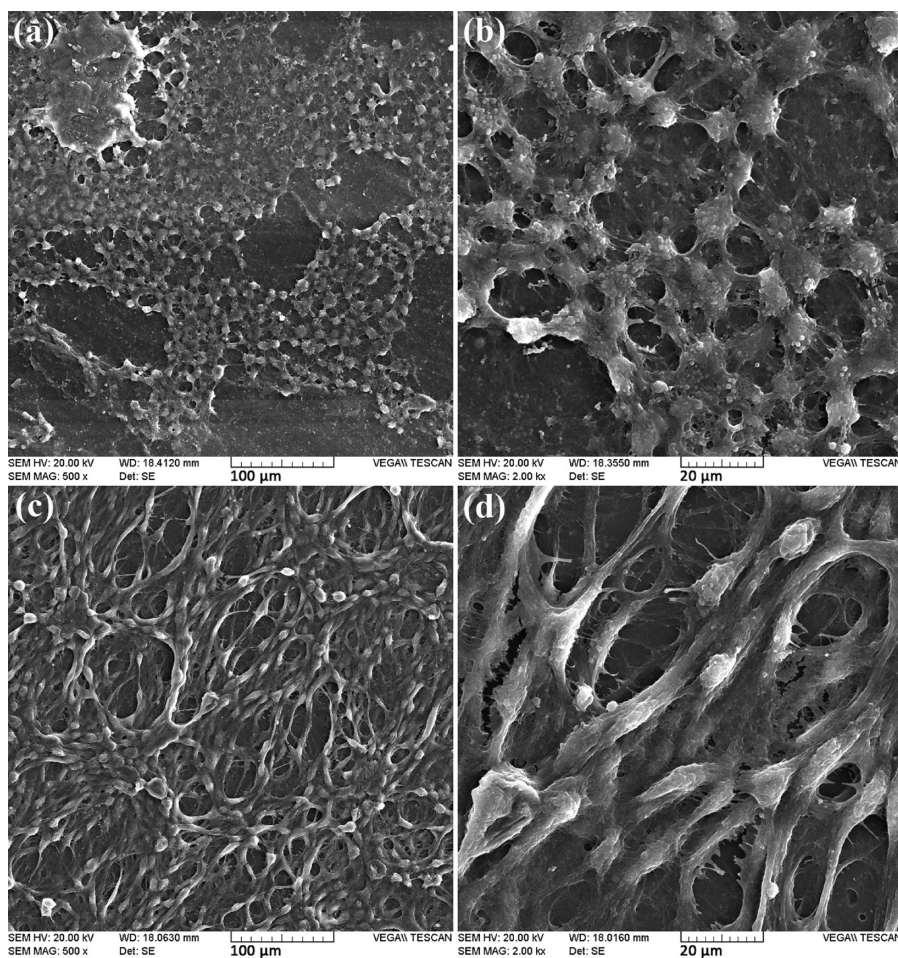


**Figure 4.** SEM images of fixed L929 mouse fibroblast cells adhered to washed polyurethanes after 24 h incubation: XPU-A2 (a, b) and XPU-A3 (c, d).

moieties.<sup>61</sup> The  $T_g$  values of XPU-Bs were lower than the corresponding XPU-As as a result of their lower cross-linking density values as well as higher flexibility of ether ( $-\text{CH}_2-\text{O}-\text{CH}_2-$ ) bond incorporated within the networks. It is worth to mention that study of thermal transitions for the prepared polyurethane networks by DSC method led to similar conclusions for thermal behavior of soft segments (Supporting Information, Figure S8).

The effect of incorporation of azide and 1,2,3-triazole groups on the thermal stability of soybean oil-based functional polyols as well as polyurethane networks derived from these polyols were evaluated by TGA method in the range of 25–600 °C under nitrogen atmosphere. The TGA and DTGA curves are illustrated in Figure 2. As it is clear from Figure 2, parts a and b, 1,2,3-triazole-functionalized polyol (SP2) showed higher thermal stability than azidated soybean oil (SP1). SP1 showed a multistep thermal degradation profile at peak temperatures of 110, 230, 385, and 455 °C. The weight loss at lower temperatures was attributed to thermal degradation of thermally labile azide moieties,<sup>54,62</sup> and the other weight losses at higher temperatures were related to thermal degradation of aliphatic hydrocarbon structure of the oil backbone.<sup>63,64</sup> Although low initial decomposition temperature was recorded for SP1, its overall rate of weight loss was also low. The generation of reactive nitrene species,<sup>52–54</sup> production of partially cross-linked soybean oil moieties, and damping of thermal energy by these extra bonds were responsible for the

low thermal degradation rate of SP1. To confirm this hypothesis, TGA data of MSP<sup>18</sup> were compared (Figure 2a,b). Much higher initial decomposition temperature was obtained for MSP. But the thermal decomposition rate of MSP was much higher than SP1, since there was no extra cross-linking reaction possible for it. SP2 showed a one-step thermal degradation profile with maximum degradation temperature at 405 °C. Conversion of the azide moieties in SP1 to thermally stable 1,2,3-triazole groups in SP2 through cycloaddition reaction improved the initial decomposition temperature of SP2, considerably. This material showed only 7% weight loss up to 300 °C.

The thermal stability data of XPU-As are compared in Figures 2c,d. It appears that the polyurethanes must have undergone a multistep thermal degradation with lower thermal stability compared to related soybean oil-based functional polyols due to formation of thermal labile urethane bonds.<sup>65,66</sup> Urethanes are known to be relatively thermally unstable materials.<sup>67,68</sup> The introduced urethane bonds resulted in the first weight loss at 308–338 °C for XPU-As. The intensity of this step was highest for XPU-A3 containing higher urethane bonds (Figure 2d). Decomposition of the urethane bonds led to the formation of *primary* amine and olefin or the formation of *secondary* amine and carbon dioxide.<sup>66</sup> The next steps of thermal degradation with peak temperatures at 382–390 and 427–442 °C were related to the thermal degradation of aliphatic hydrocarbon structure of un-cross-linked and cross-

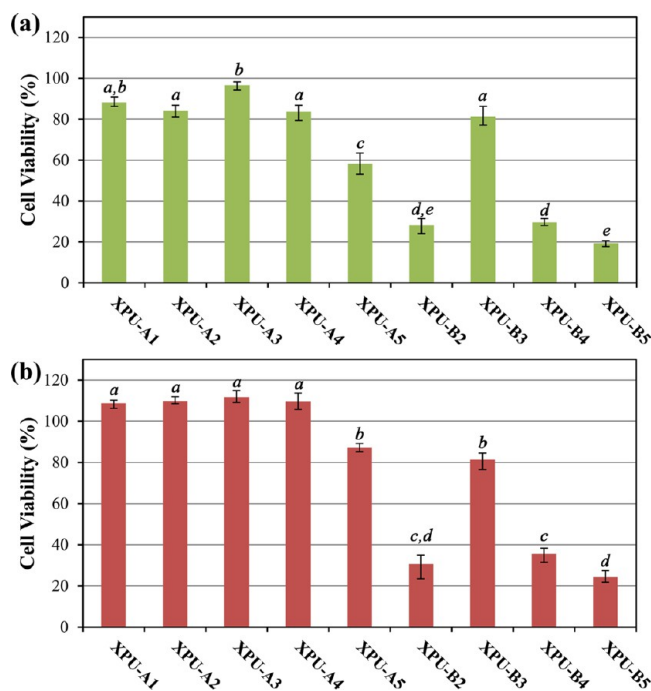


**Figure 5.** Cell viability of L929 mouse fibroblast cells in direct contact with polyurethanes (a) and their extracted leachates in growth media (b). According to analysis of variances the difference between quantities with similar superscripts (a, b, c, d and e) is not significant ( $p > 0.05$ ).

**Table 4.** Antibacterial and Antifungal Activities of Polyols and Polyurethanes<sup>a</sup>

sample code	inhibition zone (mm)			microorganism reduction (%)		
	<i>E. coli</i>	<i>S. aureus</i>	<i>C. albicans</i>	<i>E. coli</i>	<i>S. aureus</i>	<i>C. albicans</i>
SP1	0	0	2.7	2.7	0.0	2.2
SP2	0	0	0.0	0.0	0.0	0.0
SP3	0	0.6	1.1	0.0	0.0	0.0
SP4	0	1.5	2.9	16.3	22.9	77.1
SP5	2.2	2.5	4.7	88.1	100.0	100.0
XPU-A1	0.0	0.0	0.0	0.0	8.8	4.5
XPU-A2	0.0	0.0	0.0	0.0	13.8	7.7
XPU-A3	0.0	0.0	0.0	0.0	14.8	9.0
XPU-A4	0.0	0.0	0.0	0.4	32.3	25.4
XPU-A5	0.0	0.0	0.0	81.0	86.0	88.9
XPU-B2	0.0	0.0	0.0	0.0	10.8	11.3
XPU-B3	0.0	0.0	0.0	0.0	10.3	6.7
XPU-B4	0.0	0.0	0.0	0.0	36.1	50.3
XPU-B5	0.0	0.0	0.0	92.0	99.1	100.0
DMF	0.0	0.0	0.3	0.0	0.0	0.0
CT 30 <sup>b</sup>	7.0	5.4	—	—	—	—

<sup>a</sup>Polyurethanes were washed and extracted with ethanol/water mixture (70:30 v/v) for one week. <sup>b</sup>Ceftizoxime (30 µg/disc).

linked moieties of soybean oil.<sup>65,66</sup> Weight loss observed at 248 °C for XPU-A1 was related to thermal degradation of azide moieties. Moreover, QAS-containing polyurethane (XPU-A5) showed lower thermal stability compared to other samples. This phenomenon could be related to thermal decomposition of incorporated QAS (alkyltrimethylammonium iodide and 3-methyl-1,2,3-triazolium iodide) moieties.<sup>55–60</sup> QAS groups are known to decompose through combination of dealkylation and Hoffman elimination mechanisms.<sup>55,56,58</sup> Furthermore, TGA

results suggested that, in comparison to XPU-A4, the presence of the QAS groups accelerated the decomposition of polyurethane backbone.

**3.4. Surface and Bulk Hydrophilicity of XPUs.** Surface hydrophilicity is a determining factor for microorganism adhesion on the surface of materials.<sup>69</sup> In course of antibacterial and antifungal action of biocidal polymeric coatings, the microorganism should spread and come into contact with biocidal moieties chemically anchored on the coating surface. Therefore, hydrophilic biocidal coatings show more activity against microorganisms such as *E. coli*, *S. aureus*, and *C. albicans*, which are hydrophilic under physiological condition.<sup>70,71</sup> The surface and bulk hydrophilicity of prepared polyurethanes were studied through measurement of their static water contact angle and the amount of equilibrium absorbed water with either distilled water or PBS. The results are collected in Table 3. The surface of all polyurethanes were considered as moderately hydrophilic, since their water contact angle values were in the range of 43–83 degree. XPU-A1 containing azide moieties showed higher hydrophilicity ( $\theta = 43^\circ$ ) in comparison to other XPUs. Moreover, the higher surface hydrophilicity (lower water contact angle) for XPU-A4 and XPU-A5 compared to XPU-A2 and XPU-A3 were related to their incorporated hydrophilic tertiary amine and QAS (alkyltrimethylammonium iodide and 3-methyl-1,2,3-triazolium iodide) groups, respectively. As expected, all of polyurethanes which consisted of PEG1000 showed higher surface hydrophilicity in comparison to those corresponding formulations made entirely from soybean oil-based functional polyol. This phenomenon was due to the ability of ether moieties of PEG1000 to form hydrogen bonding with water molecules.

According to Table 3, the trend for EWA was similar to what observed for contact angle values. It is interesting that the EWA values were lower in PBS (1.2–82.3%) than distilled water (1.5–104.6%). This phenomenon is attributed to higher ionic strength of the PBS medium containing NaCl,  $\text{KH}_2\text{PO}_4$ ,  $\text{Na}_2\text{HPO}_4$  salts. Increasing the ionic strength reduces the osmotic swelling pressure as the main driving force for absorption of water into the polymer.<sup>72,73</sup> It is emphasized that exposing polar active functions chemically anchored into the prepared polyurethane networks is much higher in polar media. Therefore, it is expected that samples with higher surface and bulk hydrophilicity show higher biological activities.

**3.5. Hardness and Adhesion of XPUs.** Since the application of these new polyurethanes was intended in surface coatings for biomedical implants and devices, hardness and adhesion strength as most routine criteria for coating application were measured. The pendulum hardness values of polyurethanes are given in Table 3. As expected, XPU-A3 showed the highest hardness between XPUs. This result is in accordance to DMA data, which XPU-A3 with the highest cross-link density showed the lowest  $\tan \delta$  values (lowest damping factor). According to Table 3, XPU-A5 showed higher hardness compared to XPU-A2 and XPU-A4. This can be attributed to ionic interactions of QAS (alkyltrimethylammonium iodide and 3-methyl-1,2,3-triazolium iodide) moieties in the backbone of XPU-A5. Moreover, polyurethanes consisting PEG1000 (XPUs-Bs) showed lower hardness compared to those corresponding formulations made entirely from soybean oil-based functional polyol (XPUs-As). This phenomenon was again in agreement with DMA data, in which XPU-B2 and XPU-B4 showed higher  $\tan \delta$  values (lower damping factor) compared to XPU-A2 and XPU-A4.



The adhesion strength of XPU-As coatings spread over surface-treated aluminum plate was measured by pull-off adhesion test. The results are collected in Table 3. The polyurethane coatings showed adhesion strength in the range of 0.14–0.43 MPa depending on type of functional polyols used for their preparation. XPU-A5 showed the highest adhesion strength among other XPU-As. This finding could be related to the incorporated QAS (alkyltrimethylammonium iodide and 3-methyl-1,2,3-triazolium iodide) moieties within the backbone of polymer chains, which led to increased Coulombic attraction of coating material and substrate. This phenomenon was in agreement with our previous results<sup>17,18</sup> and some reports about adhesion promoting property of polymeric and low molecular weight quaternary alkyl ammonium compounds<sup>74,75</sup> and improved adhesion strength of polyurethane cationomers to glass, aluminum and PVC substrates.<sup>76,77</sup>

**3.6. Cytocompatibility of XPUs.** Cytocompatibility of polyurethanes was studied by the evaluation of their interaction with L929 mouse fibroblast cells via either microscopic investigation of cells morphology or MTT assay. Such a study is required to gain insight into the suitability of these materials for biomedical applications. Samples were washed and extracted with ethanol/water mixture (70:30 v/v) to remove all nonbonded compounds. Optical microscopic images of XPU-As cultured with fibroblast cells are given in Figure 3. The evaluation of cell morphology showed cells survived and grew with spindle shape morphology and none of the prepared polyurethanes appeared to give off any toxic or inhibitory leachates, since cells grew to confluence on all samples. Representative SEM image of XPU-A2 and XPU-A3 with fixed attached fibroblast cells are also presented in Figure 4. These SEM images confirmed excellent adhesion and flattening of fibroblast cells onto the samples surface. Therefore, based on qualitative cell morphology inspection, the level of cytocompatibility for XPU-As was acceptable. For better judgment, the cytocompatibility of samples was determined via quantitative MTT assay.

The MTT assay was carried out on the fibroblast cells in contact with either polyurethane films or their extracted leachates in growth medium. The cell viability values are collected in Figure 5. For XPU-As, MTT assay showed cell viability values in the range of 60–110% demonstrating cytocompatibility (nontoxicity) of the prepared polyurethanes. It is worth to mention that QAS-containing sample (XPU-A5) showed lower cell viability in comparison to other XPU-As. This observation is in agreement with our previous results.<sup>17,18</sup> In practice, evaluation of in vitro cytotoxicity showed some sort of cytotoxic effect for high concentration of QAS.<sup>78,79</sup> Another possible explanation for this phenomenon is attributed to partial instability of iodide anions of incorporated QAS (alkyltrimethylammonium iodide and 3-methyl-1,2,3-triazolium iodide) moieties,<sup>80</sup> which can produce small amounts of toxic materials such as iodine and hydrogen iodide.<sup>81,82</sup> On the basis of the above results, the acceptable cytocompatibility of XPU-As was confirmed.

Considerable reduction of cytocompatibility was observed for polyurethanes containing PEG1000 in their formulations (XPU-Bs). PEG1000 itself is a biologically safe material. However, due to lower cross-link density and higher surface and bulk hydrophilicity of polyurethane networks containing PEG1000, higher chance for interaction of cells with QAS and 1,2,3-triazole groups may occur in aqueous medium. Therefore, due to partial toxicity of these functional groups, a relatively

lower cytocompatibility was nevertheless observed for XPU-Bs. It is interesting to note that XPU-B3, the sample with the highest cross-link density of network and therefore more immobilized active functional groups, demonstrated better cytocompatibility within XPU-Bs.

### 3.7. Antibacterial and Antifungal Activities of XPUs.

Antibacterial and antifungal activities of low-molecular weight 1,2,3-triazole derivatives have been reported.<sup>22–25</sup> Evaluation of biocidal activity of high-molecular weight analogous of 1,2,3-triazole compounds due to the presence of these functional groups have been considered in the present study. For this purpose, the possible biocidal activity of 1,2,3-triazole-containing polyols and the corresponding polyurethanes was examined against *E. coli*, *S. aureus*, and *C. albicans* through agar diffusion and shaking flask methods (Table 4). No inhibition zone was observed for SP1 against both of studied bacteria; however, an inhibition zone of 2.7 mm was observed for *C. albicans*. On the basis of agar diffusion test, no considerable inhibition zone was detected for 1,2,3-triazole-functionalized polyols (SP2–SP4). Meanwhile, SP3 and SP4 with hydrophilic hydroxyl and tertiary amine groups showed small inhibition zones. Agar diffusion results showed that antifungal activity of these polyols (SP2–SP4) was partially better than their antibacterial activity (Table 4). As expected, incorporation of QAS (alkyltrimethylammonium iodide and 3-methyl-1,2,3-triazolium iodide) moieties within oil backbone (SP5) provided inhibition zones against all microorganisms. Quantitative evaluation of biocidal property of polyols by shaking flask method showed promising antifungal and low to moderate antibacterial activities for SP4 and SP5, respectively. It seems that the incorporation of 1,2,3-triazole groups within the oil backbone cannot by themselves provide a considerable biocidal activity. Furthermore, biocidal activity of SP4 could be attributed to the presence of tertiary amine groups with possible protonated residues.<sup>83</sup>

Antibacterial and antifungal activities of polyurethanes prepared from functional polyols were also investigated. According to Table 4, washed polyurethanes showed no inhibition zone for all microorganisms, which confirmed that all biocidal functions were covalently attached to the backbone of polymer chains. No biocidal effects were observed for azide-containing polyurethane (XPU-A1) as well as those containing only 1,2,3-triazole groups (XPU-A2 and XPU-A3). However, polyurethanes containing tertiary amine and QAS groups (XPU-A4 and XPU-A5) showed moderate to high biocidal activity against microorganisms specially *S. aureus* and *C. albicans*. Partial improvement of biocidal activity was detected for polyurethanes containing PEG1000. Higher hydrophilicity of these samples and their more efficient interaction of anchored biocidal groups with microorganisms were responsible for this improvement.

## 4. CONCLUSION

Novel 1,2,3-triazole-functionalized soybean oil-based polyols were synthesized and used for the preparation of polyurethane coatings. In comparison to azide-containing polyurethane, incorporation of 1,2,3-triazole groups within the polyol backbone caused considerable improvement of modulus at glassy state, glass transition temperature, thermal stability and hardness of the corresponding polyurethane coatings. In contrast, the adhesion strength and hydrophilicity of the polyurethanes containing heterocyclic ring were decreased. Although QAS-containing polyurethane networks displayed



better modulus at glassy state, but their glass transition temperature, hydrophilicity, hardness and adhesion strength, and their thermal stability were reduced. Studying the interaction of fibroblast cells with polyurethanes made merely from oil-based polyols revealed good cells viability in the range 60–110%. Moderate to high biocidal activity was detected for polyols containing tertiary amine and QAS groups as well as their corresponding polyurethanes. Improving hydrophilicity of polyurethane networks via incorporation of PEG1000 improved their biocidal activity, while reduced their cytocompatibility.

## ■ ASSOCIATED CONTENT

### ■ Supporting Information

Additional data related to prepared polyols and polyurethanes. This material is available free of charge via the Internet at <http://pubs.acs.org/>.

## ■ AUTHOR INFORMATION

### Corresponding Author

\*(H.Y.) Telephone: +98-21-48662447. Fax: +98-21-44580021. E-mail: [h.yeganeh@ippi.ac.ir](mailto:h.yeganeh@ippi.ac.ir).

### Notes

The authors declare no competing financial interest.

## ■ REFERENCES

- (1) Chattopadhyay, D. K.; Raju, K. V. S. N. *Prog. Polym. Sci.* **2007**, *32*, 352–418.
- (2) Petrovic, Z. S. *Polym. Rev.* **2008**, *48*, 109–155.
- (3) Yeganeh, H.; Shamekhi, M. A. *J. Appl. Polym. Sci.* **2006**, *99*, 1222–1233.
- (4) Ronda, J. C.; Lligadas, G.; Galia, M.; Cadiz, V. *Eur. J. Lipid Sci. Technol.* **2011**, *113*, 46–58.
- (5) Yeganeh, H.; Hojati-Talemi, P. *Polym. Degrad. Stab.* **2007**, *92*, 480–489.
- (6) Petrovic, Z. S.; Guo, A.; Javni, I.; Cveticovic, I.; Hong, D. P. *Polym. Int.* **2008**, *57*, 275–281.
- (7) Guo, A.; Zhang, W.; Petrovic, Z. S. *J. Mater. Sci.* **2006**, *41*, 4914–4920.
- (8) Guo, A.; Cho, Y.; Petrovic, Z. S. *J. Polym. Sci., Part A: Polym. Chem.* **2000**, *38*, 3900–3910.
- (9) Khot, S. N.; Lascala, J. J.; Can, E.; Morye, S. S.; Williams, G. I.; Palmese, G. R.; Kusefoglu, S. H.; Wool, R. P. *J. Appl. Polym. Sci.* **2001**, *82*, 703–723.
- (10) Chen, Z.; Chisholm, B. J.; Patani, R.; Wu, J. F.; Fernando, S.; Jogodzinski, K.; Webster, D. C. *J. Coat. Technol. Res.* **2010**, *7*, 603–613.
- (11) Biermann, U.; Linker, U.; Metzger, J. O. *Eur. J. Lipid Sci. Technol.* **2013**, *115*, 94–100.
- (12) Adewuyi, A.; Göpfert, A.; ThomasWolff; Rao, B. V. S. K.; Prasad, R. B. N. *ISRN Org. Chem.* **2012**, *2012*, 1–7.
- (13) Biswas, A.; Sharma, B. K.; Willett, J. L.; Advaryu, A.; Erhan, S. Z.; Cheng, H. N. *J. Agric. Food Chem.* **2008**, *56*, 5611–5616.
- (14) Furmeier, S.; Metzger, J. O. *Eur. J. Org. Chem.* **2003**, *2003*, 649–659.
- (15) Metzger, J. O.; Furmeier, S. *Eur. J. Org. Chem.* **1999**, *1999*, 661–664.
- (16) Metzger, J. O.; Linker, U. *Fat Sci. Technol.* **1991**, *93*, 244–249.
- (17) Bakhshi, H.; Yeganeh, H.; Mehdipour-Ataei, S.; Shokrgozar, M. A.; Yari, A.; Saeedi-Eslami, S. N. *Mater. Sci. Eng., C* **2013**, *33*, 153–164.
- (18) Bakhshi, H.; Yeganeh, H.; Mehdipour-Ataei, S. *J. Biomed. Mater. Res. Part A* **2013**, *101A*, 1599–1611.
- (19) Jalilian, M.; Yeganeh, H.; Haghighi, M. N. *Polym. Adv. Technol.* **2010**, *21*, 118–127.
- (20) Jalilian, M.; Yeganeh, H.; Haghighi, M. N. *Polym. Int.* **2008**, *57*, 1385–1394.
- (21) Qin, A.; Lam, J. W. Y.; Tang, B. Z. *Macromolecules* **2010**, *43*, 8693–8702.
- (22) Demaray, J. A.; Thuener, J. E.; Dawson, M. N.; Sucheck, S. J. *Bioorg. Med. Chem. Lett.* **2008**, *18*, 4868–4871.
- (23) Reck, F.; Zhou, F.; Girardot, M.; Kern, G.; Eyermann, C. J.; Hales, N. J.; Ramsay, R. R.; Gravestock, M. B. *J. Med. Chem.* **2005**, *48*, 499–506.
- (24) Tian, L.; Sun, Y.; Li, H.; Zheng, X.; Cheng, Y.; Liu, X.; Qian, B. *J. Inorg. Biochem.* **2005**, *99*, 1646–1652.
- (25) Holla, B. S.; Mahalinga, M.; Karthikeyan, M. S.; Poojary, B.; Akberali, P. M.; Kumari, N. S. *Eur. J. Med. Chem.* **2005**, *40*, 1173–1178.
- (26) Alvarez, R.; Vázquez, S.; San-Félix, A.; Aquaro, S.; De Clercq, E.; Perno, C. F.; Karlsson, A.; Balzarini, J.; Camarasa, M. J. *J. Med. Chem.* **1994**, *37*, 4185–4194.
- (27) Buckle, D. R.; Outred, D. J.; Rockell, C. J. M.; Smith, H.; Spicer, B. A. *J. Med. Chem.* **1983**, *26*, 251–254.
- (28) Malkoch, M.; Schleicher, K.; Drockenmuller, E.; Hawker, C. J.; Russell, T. P.; Wu, P.; Fokin, V. V. *Macromolecules* **2005**, *38*, 3663–3678.
- (29) Gierlich, J.; Burley, G. A.; Gramlich, P. M. E.; Hammond, D. M.; Carell, T. *Org. Lett.* **2006**, *8*, 3639–3642.
- (30) Breed, D. R.; Thibault, R.; Xie, F.; Wang, Q.; Hawker, C. J.; Pine, D. J. *Langmuir* **2009**, *25*, 4370–4376.
- (31) O'Reilly, R. K.; Joralemon, M. J.; Wooley, K. L.; Hawker, C. J. *Chem. Mater.* **2005**, *17*, 5976–5988.
- (32) Li, Y.; Santos, C. M.; Kumar, A.; Zhao, M.; Lopez, A. I.; Qin, G.; McDermott, A. M.; Cai, C. *Chem.—Eur. J.* **2011**, *17*, 2656–2665.
- (33) Wang, B.; Liu, M.; Chen, Z.; Liang, R.; Ding, S.; Chen, S.; Jin, S. *Int. J. Pharm.* **2007**, *331*, 19–26.
- (34) Riva, R.; Lussis, P.; Lenoir, S.; Jerome, C.; Jerome, R.; Lecomte, P. *Polymer* **2008**, *49*, 2023–2028.
- (35) Anthierens, T.; Billiet, L.; Devlieghere, F.; Prez, F. D. *Innov. Food Sci. Emerg. Technol.* **2012**, *15*, 81–85.
- (36) Thomassin, J.-M.; Lenoir, S.; Riga, J.; Jerome, R.; Detrembleur, C. *Biomacromolecules* **2007**, *8*, 1171–1177.
- (37) Hetzer, M.; Chen, G.; Barner-Kowollik, C.; Stenzel, M. H. *Macromol. Biosci.* **2010**, *10*, 119–126.
- (38) Thibault, R. J.; Takizawa, K.; Lowenheim, P.; Helms, B.; Mynar, J. L.; Frechet, J. M. J.; Hawker, C. J. *J. Am. Chem. Soc.* **2006**, *128*, 12084–12085.
- (39) Besset, C.; Pascault, J.-P.; Fleury, E.; Drockenmuller, E.; Bernard, J. *Biomacromolecules* **2010**, *11*, 2797–2803.
- (40) Binauld, S.; Boisson, F.; Hamaide, T.; Pascault, J.-P.; Drockenmuller, E.; Fleury, E. *J. Polym. Sci. Part A Polym. Chem.* **2008**, *46*, 5506–5517.
- (41) Johnson, J. A.; Lewis, D. R.; Díaz, D. D.; Finn, M. G.; Koberstein, J. T.; Turro, N. J. *J. Am. Chem. Soc.* **2006**, *128*, 6564–6565.
- (42) Li, C.; Finn, M. G. *J. Polym. Sci., Part A: Polym. Chem.* **2006**, *44*, 5513–5518.
- (43) Wu, P.; Feldman, A. K.; Nugent, A. K.; Hawker, C. J.; Scheel, A.; Voit, B.; Pyun, J.; Fréchet, J. M. J.; Sharpless, K. B.; Prof, V. V. F. *Angew. Chem., Int. Ed.* **2004**, *43*, 3928–3932.
- (44) Hong, J.; Shah, B. K.; Petrovic, Z. S. *Eur. J. Lipid Sci. Technol.* **2013**, *115*, 55–60.
- (45) Hong, J.; Luo, Q.; Wan, X.; Petrović, Z. S.; Shah, B. K. *Biomacromolecules* **2012**, *13*, 261–266.
- (46) Hong, J.; Luo, Q.; Shah, B. K. *Biomacromolecules* **2010**, *11*, 2960–2965.
- (47) Kenawy, E.; Worley, S. D.; Broughton, R. *Biomacromolecules* **2007**, *8*, 1359–1384.
- (48) Treloar, L. R. G., *The Physics of Rubber Elasticity*, 3rd ed.; Oxford University Press: London, 2009.
- (49) Yari, A.; Yeganeh, H.; Bakhshi, H.; Gharibi, R. *J. Biomed. Mater. Res. Part A* **2013**, DOI: 10.1002/jbm.a.34672.
- (50) Yari, A.; Yeganeh, H.; Bakhshi, H. *J. Mater. Sci. Mater. Med.* **2012**, *23*, 2187–2202.

- (51) Dimitrov-Raytchev, P.; Beghdadi, S.; Serghei, A.; Drockenmuller, E. *J. Polym. Sci., Part A: Polym. Chem.* **2013**, *51*, 34–38.
- (52) Damiron, D.; Okhay, N.; Al-Akhrass, S.; Cassagnau, P.; Drockenmuller, E. *J. Polym. Sci., Part A: Polym. Chem.* **2012**, *50*, 99–107.
- (53) Zielińska, A. J.; Noordermeer, J. W. M.; Talma, A. G.; Duin, M. V. *Rubber Chem. Technol.* **2011**, *84*, 243–257.
- (54) Zielińska, A. J.; Noordermeer, J. W. M.; Dierkes, W. K.; Talma, A. G.; van Duin, M. *Kautsch. Gummi Kunstst.* **2010**, *63*, 308–315.
- (55) Coneski, P. N.; Weise, N. K.; Fulmer, P. A.; Wynne, J. H. *Prog. Org. Coat.* **2013**, *76*, 1376–1386.
- (56) Coneski, P. N.; Fulmer, P. A.; Wynne, J. H. *Langmuir* **2012**, *28*, 7039–7048.
- (57) Xia, Y.; Zhang, Z.; Kessler, M. R.; Brehm-Stecher, B.; Larock, R. C. *ChemSusChem* **2012**, *5*, 2221–2227.
- (58) Wynne, J. H.; Fulmer, P. A.; McCluskey, D. M.; Mackey, N. M.; Buchanan, J. P. *ACS Appl. Mater. Interfaces* **2011**, *3*, 2005–2011.
- (59) Wang, J.; Zhao, Z.; Gong, F.; Li, S.; Zhang, S. *Macromolecules* **2009**, *42*, 8711–8717.
- (60) Kurt, P.; Wynne, K. J. *Macromolecules* **2007**, *40*, 9537–9543.
- (61) Kebir, N.; Campistron, I.; Laguerre, A.; Pilard, J. F.; Bunel, C.; Jouenne, T. *Biomaterials* **2007**, *28*, 4200–4208.
- (62) L'abbe, G. *Chem. Rev.* **1969**, *69*, 345–363.
- (63) Ahn, B. K.; Kraft, S.; Wang, D.; Sun, X. S. *Biomacromolecules* **2011**, *12*, 1839–1843.
- (64) Lin, B.; Yang, L.; Dai, H.; Hou, Q.; Zhang, L. *J. Therm. Anal. Calorim.* **2009**, *95*, 977–983.
- (65) Mohd-Rus, A. Z.; Kemp, T. J.; Clark, A. J. *Prog. React. Kinet. Mech.* **2009**, *34*, 1–41.
- (66) Javni, I.; Petrović, Z. S.; Guo, A.; Fuller, R. J. *Appl. Polym. Sci.* **2000**, *77*, 1723–1734.
- (67) Grassie, N.; Mendoza, G. A. P. *Polym. Degrad. Stab.* **1985**, *10*, 267–286.
- (68) Gaboriaud, F.; Vantelon, J. P. *J. Polym. Sci. Part A Polym. Chem.* **1982**, *20*, 2063–2071.
- (69) Pavithra, D.; Doble, M. *Biomed. Mater.* **2008**, *3*, 1–13.
- (70) Chung, Y. C.; Su, Y. P.; Chen, C. C.; Jia, G.; Wang, H. L.; Wu, J. C. G.; Lin, J. G. *Acta Pharmacol. Sin.* **2004**, *25*, 932–936.
- (71) Bruinsma, G. M.; Mei, H. C. v. d.; Busscher, H. J. *Biomaterials* **2001**, *22*, 3217–3224.
- (72) Zhao, Y.; Kang, J.; Tan, T. *Polymer* **2006**, *47*, 7702–7710.
- (73) Lee, W.-F.; Lin, G.-H. *J. Appl. Polym. Sci.* **2001**, *79*, 1665–1674.
- (74) McGee, D. E. Cationic, amino-functional, adhesion-promoting polymer for curable inks and other plastic film coatings, and plastic film comprising such polymer. 6,893,722, 2005.
- (75) Wilson, J.; Tabb, D. L. Fluoroelastomer compositions containing a tetraalkylammonium metal adhesion promoter. EP0420662, 1995.
- (76) Malavasic, T.; Cernilec, N.; Mirceva, A.; Osredkar, U. *Int. J. Adhes. Adhes.* **1992**, *12*, 38–42.
- (77) Hsu, S. L.; Xiao, H. X.; Szmant, H. H.; Frisch, K. C. *J. Appl. Polym. Sci.* **1984**, *29*, 2467–2479.
- (78) Stratton, T. R.; Rickus, J. L.; Youngblood, J. P. *Biomacromolecules* **2009**, *10*, 2550–2555.
- (79) Fischera, D.; Li, Y.; Ahlemeyer, B.; Kriegelstein, J.; Kissel, T. *Biomaterials* **2003**, *24*, 1121–1131.
- (80) Domard, A.; Rinaudo, M.; Terrassin, C. *Int. J. Biol. Macromol.* **1986**, *8*, 105–107.
- (81) Biber, F. Z.; Unak, P.; Yurt, F. *Isotopes Environ. Health Stud.* **2002**, *38*, 87–93.
- (82) Diosady, L. L.; Alberti, J. O.; Mannar, M. G. V.; FitzGerald, S. *Food Nutr. Bull.* **1998**, *19*, 240–250.
- (83) Endo, Y.; Tani, T.; Kodama, M. *Appl. Environ. Microbiol.* **1987**, *53*, 2050–2055.